Nanotechnology

Uniformly coated highly porous graphene/MnO_2 foams for flexible supercapacitors

To cite this article before publication: Simon Drieschner *et al* 2018 *Nanotechnology* in press https://doi.org/10.1088/1361-6528/aab4c2

Uniformly coated highly porous graphene/MnO_2 foams for flexible asymmetric supercapacitors

Simon Drieschner[1], Maximilian von Seckendorff[1], Elena del Corro[2], Jörg Wohlketzetter[1], Benno M. Blaschke[1], Martin Stutzmann[1], and Jose A. Garrido[2,3]

[1]Walter Schottky Institut und Physik-Department, Technische Universität München, Am Coulombwall 4, 85748 Garching, Germany

[2]ICN2 – Catalan Institute of Nanoscience and Nanotechnology, Barcelona Institute of Science and Technology and CSIC, Campus UAB, 08193 Bellaterra, Spain

[3]ICREA, Institució Catalana de Recerca i Estudis Avançats, 08070 Barcelona, Spain

E-mail: joseantonio.garrido@icn2.cat

Abstract.

Supercapacitors are called to play a prominent role in the newly emerging markets of electric vehicles, flexible displays and sensors, and wearable electronics. In order to compete with current battery technology, supercapacitors have to be designed with highly conductive current collectors exhibiting high surface area per unit volume and uniformly coated with pseudocapacitive materials, which is crucial to boost the energy density while maintaining a high power density. Here, we present a versatile technique to prepare thickness-controlled thin-film micro graphene foams (µGFs) with pores in the lower micrometer range grown by chemical vapor deposition which can be used as highly conductive current collectors in flexible supercapacitors. To fabricate the µGF, we use porous metallic catalytic substrates consisting of nickel/copper alloy synthesized on nickel foil by electrodeposition in an electrolytic solution. Changing the duration of the electrodeposition allows the control of the thickness of the metal foam, and thus of the µGF, ranging from a few micrometers to the millimeter scale. The resulting µGF with a thickness and pores in the micrometer regime exhibits high structural quality which leads to a very low intrinsic resistance of the devices. Transferred onto flexible substrates, we demonstrate a uniform coating of the µGFs with manganese oxide, a pseudocapacitively active material. Considering the porous structure and the thickness of the µGFs, square wave potential pulses are used to ensure uniform coverage by the oxide material boosting the volumetric and areal capacitance to $14\,\mathrm{F\,cm^{-3}}$ and $0.16\,\mathrm{F\,cm^{-2}}$. The µGF with a thickness and pores in the micrometer regime in combination with a coating technique tuned to the porosity of the µGF is of great relevance for the development of supercapacitors based on state-of-the-art graphene foams.

Keywords: graphene foams, electrodeposition, CVD, asymmetric supercapacitor

Submitted to: *Nanotechnology*

1. Introduction

The growing demand for energy and the push to use less contaminating energy sources has boosted the exploration of environmentally friendly and clean energy sources. The increasing involvement of renewable energy sources requires more efficient energy storage systems since the energy supply from some of these energy sources, e.g. solar and wind energy, can vary significantly over short periods of time and, therefore, cannot be exploited evenly and consistently. Supercapacitors, energy storage devices with a much higher power density than batteries[1], have attracted significant attention since they can store and provide energy within very short times, outperforming batteries in many electrical and thermal parameters as well as in safety and cost issues[2]. Whereas the energy figure of merit is typically characterized by the capacitance, the power density is generally limited by the equivalent series resistance (ESR) of the device. The ESR is the internal resistance that appears in series with the capacitor and describes the Ohmic losses during the operation of the capacitor. The capacitance of supercapacitors consists of the electric double layer capacitance and the pseudocapacitance[2]. The energy in an electric double layer capacitor (EDLC) is stored by the separation of charge between the electrode's surface and the ions in the electrolyte, while the storage mechanism in pseudocapacitors is based on fast reversible chemical reactions at the electrodes' surface[3]. In order to harness and maximize the advantages of supercapacitors, it is necessary to develop porous materials yielding high capacitance values per unit volume with a highly conductive current collector. Graphene foams, three-dimensional interconnected structures consisting of graphene sheets, exhibit a high surface area per unit mass in combination with a high electrical conductivity, making them attractive for electric double layer capacitors or for current collectors in asymmetric capacitors based on electrodes with pseudocapacitively active devices. There are many reports on the fabrication of flexible foams based on carbon black[4], carbon nanotubes[5], graphene hydrogel[6] or reduced graphene oxide (rGO)[7, 8, 9, 10, 11]. However, the relatively low intrinsic electrical conductivity[12, 13] of the resulting films based on these materials leads to a high intrinsic resistance, strongly compromising the performance of energy storage devices based on these materials. Ying Tao et al. report[14] on the fabrication of porous highly dense films based on a hydrothermal treatment and evaporation-induced drying of rGO with very high volumetric capacitance values up to $376\,\mathrm{F\,cm^{-1}}$. However, its potential use in flexible electronics is not discussed. In contrast to the fabrication requirements of pseudocapacitive foams with large pores ($\geq 200\,\mu\mathrm{m}$)[15, 16], foams with pores in the lower micrometer range require fine-tuned deposition techniques assuring a uniform coating of the current collector. Chemical synthesis of manganese oxide[17] might clog small pores, diminishing the accessibility to more interior pores; on the other hand, potentiostatic or galvanostatic[9] electrodeposition can result in the depletion of manganese in pores far away from the bulk of the electrolyte. Reports of coating techniques based on square wave potentiostatic pulses[18, 19, 20] use planar substrates and can not be applied to three-

dimensional structures with pores in the lower micrometer range. In fact, the coating of three-dimensional carbon structures with micrometer-sized pores ($< 10\,\mu m$) using these techniques has not been reported so far since the small pore volume easily leads to a depletion of the pseudocapacitive element in the electrolyte yielding a non-uniform coverage of the 3D structure. The published high quality graphene foams coated with pseudocapacitive materials[15, 16, 21, 22, 23, 24, 25, 26, 27, 28, 29, 30] are all based on mm-thick commercially available metal substrates with pore sizes larger than $200\,\mu m$ and do not show pores in the lower micrometer range[31], which would complicate a uniform coverage of the graphene foam current collector. Furthermore, they suffer from low volumetric capacitances and, thus, low energy densities, since their large pores do not contribute to the energy storage, strongly compromising their use in real application. The large thickness of these coated graphene foams limits their use in flexible energy storage devices. Other works reporting the coating of porous metallic structures (without using graphene) are also based on commercially available metal foams with pores larger than $200\,\mu m$ [32, 33, 34, 35, 36]. Further reports demonstrating the fabrication of flexible supercapacitors consisting of mechanically stable graphene-based electrodes such as rGO in combination with PANI[37], PPy[38], or $Ni(OH)_2$[39], or graphene paper with MnO_2[40] or $NiCo_2O_4$[41] show high capacitance values. However, a low long-term stability or a high intrinsic resistance strongly limit their electrochemical performance and their use in real application.

Here, we report a method for the fabrication of flexible thin-film micro graphene foams (µGFs) consisting of high quality graphene grown by chemical vapor deposition (CVD) uniformly coated with manganese oxide. The metal catalyst used as substrate for graphene growth is created by potentiostatic electrodeposition of Ni and Cu on Ni foil, yielding an interconnected three-dimensional NiCu alloy characterized by pores in the lower micrometer and sub-micrometer range. After CVD growth of few layer graphene using methane as carbon source and the removal of the metal in a wet-etching process, a high quality thin-film µGF is obtained and transferred to a flexible polyester substrate PEN. The thickness of this foam can be tuned by the duration of the electrodeposition of the NiCu alloy. The µGF is then coated with manganese oxide using square wave potential pulses whose duty cycle is tuned to the porous substrate structure, aiming at preventing the depletion of manganese in pores with long paths to the electrolyte bulk. The as-obtained electrode is used as the cathode in an asymmetric supercapacitor fabricated with a second highly conductive bare graphene foam (GF) as the anode.

2. Results and discussion

The main fabrication steps of µGFs are illustrated in Fig. 1 (left) together with scanning electron microscope (SEM) images (right). Ni foil ($25\,\mu m$ thickness, Fig. 1b) is immersed in an electrolyte (Fig. 1a (left)) containing nickel sulfate and copper sulfate. Under anodic potentiostatic conditions (see Methods for details), Ni and Cu atoms are deposited on the Ni foil leading to a porous NiCu alloy network (Fig. 1c

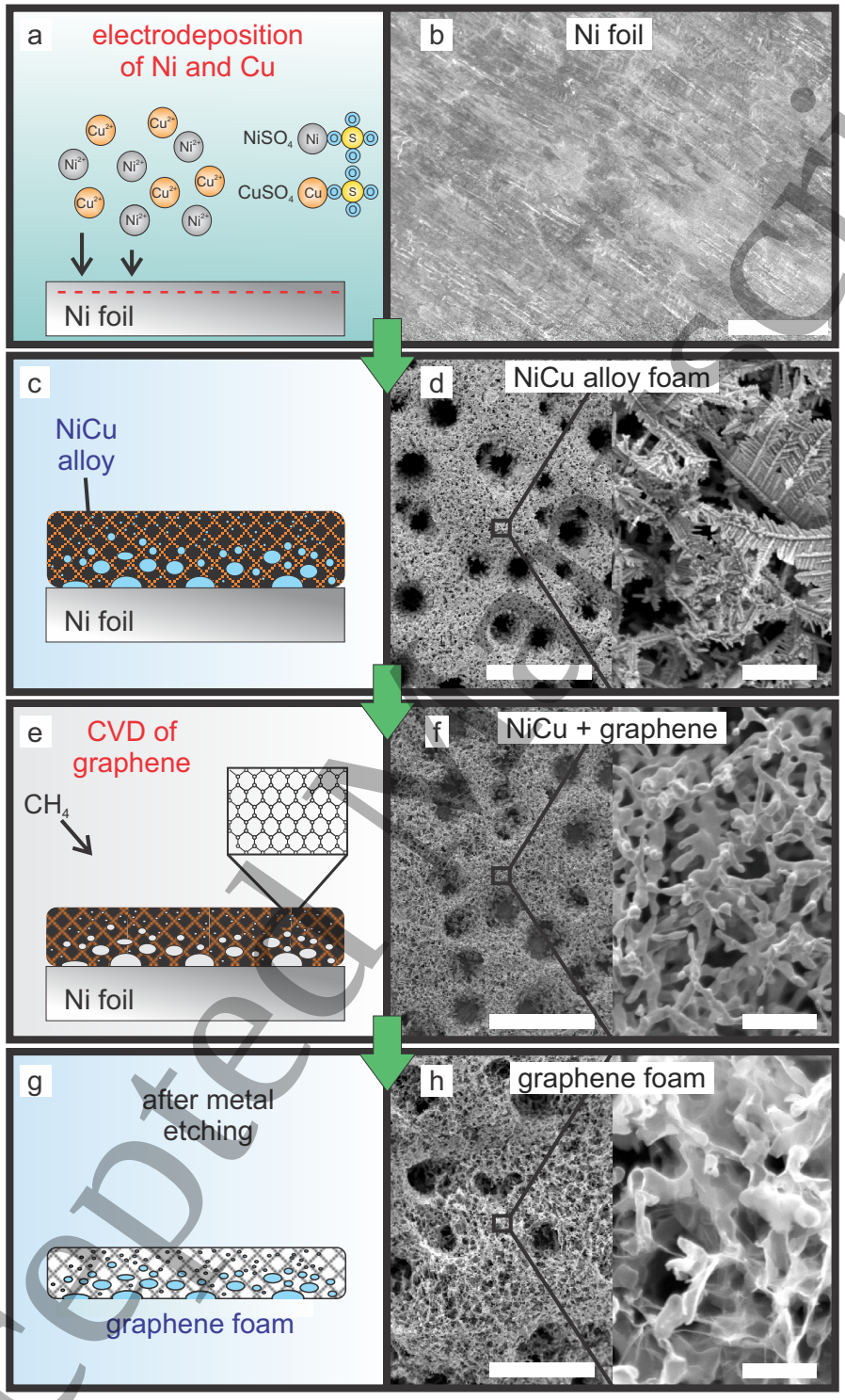

Figure 1. Illustration of the fabrication (left) of the micro graphene foams (µGFs) and scanning electron microscope images (right): a Nickel foil (b) is used as substrate for the potentiostatic electrodeposition (a) of Ni and Cu yielding a three-dimensional interconnected NiCu alloy (c, d). This scaffold serves as substrate for the growth of graphene by chemical vapor deposition using methane as carbon precursor (e, f). After etching the metal, a µGF is obtained (g, h). The scale bars in the SEM images are (b) 10 µm and (d,f,h) 100 µm (left) and 5 µm (right).

and d) as reported elsewhere[42]. The estimated ratio between Ni and Cu in the alloy is 3:2 (see Supporting Information (S.I.) for chemical element analysis). The hydrogen bubbles that are created during the deposition process (applied potential is well above the water splitting level) prevent the creation of a dense metal layer, forming instead a porous NiCu alloy structure. The size of these pores is correlated to the gas accumulated on and near the metal surface[43]. In addition to the small pores created in-between the dendrite structured metal deposits (Fig. 1d (left)), larger pores ($\geq 10\,\mu m$, Fig.1d (right)) are formed when gas bubbles merge together[44]. The porous metal substrate is then used for the growth of graphene by CVD using methane as carbon source[45, 46, 47, 48] (Fig. 1e). After heating up to 800 °C at a pressure $P \approx 200\,mbar$ under hydrogen flow to remove contamination[49] and metal oxides[46], methane molecules are introduced into the reaction tube to provide the carbon source for the graphene formation. The methane molecules dehydrogenate[49] on the catalyst's surface, leading to carbon atoms that either re-evaporate, diffuse on the surface, or diffuse into the bulk of the metal substrate[49]. The in-bulk diffusion strongly depends on the carbon solubility of the metal catalyst[50, 51]. In our case, the amount of carbon dissolved in the NiCu alloy will be between the solubility of C in Cu ($\leq 4.8\,ppm$ at 800 °C)[52]) and C in Ni ($\approx 1000\,ppm$)[53]). During the cooling phase, a fraction of the dissolved carbon atoms diffuses to the substrate's surface due to its decreasing carbon solubility and forms graphene layers, in addition to the graphene film grown on the surface during the growth step[54]. As it can be observed in Fig. 1f, apart from the small metallic dendritic structure, the porous structure of the three-dimensional network does not vanish after the high temperature step. After wet-chemical etching of the NiCu scaffold, a freestanding µGF is obtained (Fig. 1g and h).

Fig. 2a depicts a SEM image of a cross-section of the metal/graphene foam on Ni foil after graphene growth. The thickness of the metal/graphene foam depends on the duration of the electrodeposition (Fig. 2b). The minimum time to obtain a metal foam covering the whole surface of the Ni foil is one minute. Shorter deposition times do not yield an interconnected foam structure but rather isolated foam domains. Increasing the electrodeposition time leads to an almost linear increase of the metal/graphene foam thickness (Fig. 2b). Thus, by adjusting the electrodeposition time of the metal alloy, an accurate control over the graphene foam thickness can be obtained while the porous structure of the metal foam remains unaffected (see Fig. S3).

Raman spectroscopy is commonly used to estimate the number of layers and to assess the graphene crystal quality[55, 56]. Fig. 2c shows a typical Raman spectrum of the graphene layers covering the NiCu alloy substrate before metal etching. An extensive statistical evaluation of confocal Raman measurements covering a volume of $10\,\mu m^3$ is presented in the S.I.. The average full width of half maximum (FWHM) of the 2D peak, which is indicative of the graphene film thickness, varies from 33 to $100\,cm^{-1}$ and suggests the presence of single and few layer graphene (FLG) in the prepared films. This is confirmed by the G and 2D peak position of $\approx 1586\,cm^{-1}$ and $\approx 2713\,cm^{-1}$, respectively. The average D to G intensity ratio is correlated to the number of defects

in the graphene layers; we obtain a value of 0.046 ± 0.017, indicating a very good layer quality. A good graphene quality is crucial to achieve a high electrical conductivity[57] and, in turn, a low internal resistance[58] of the µGF.

The electrochemical properties of a µGF (thickness $\approx 140\,\mu m$) using our method are summarized in Fig. 3. The cyclic voltammetry (CV) curves (Fig. 3a) show no redox reaction within the explored potential window from $-0.1\,V$ to $0.8\,V$ vs Ag/AgCl, as expected for EDLCs[2] and remain quasi-rectangular even at high scan rates up to $10\,V\,s^{-1}$, indicating a very low ESR (see also S.I.). This is confirmed by electrochemical impedance spectroscopy (EIS) (Fig. 3b). A characteristic frequency higher than 200 Hz separates the resistive regime (at higher frequencies) from the capacitive regime (at lower frequencies). The maximum phase shift close to $-90°$ reveals a quasi-ideal EDLC behavior[59]. The ESR, which consists of the intrinsic resistances of the foam and the electrolyte and the resistances of the wiring, the multilayer graphene substrate (see Methods), and the contact between foam and substrate[2], can be calculated from the

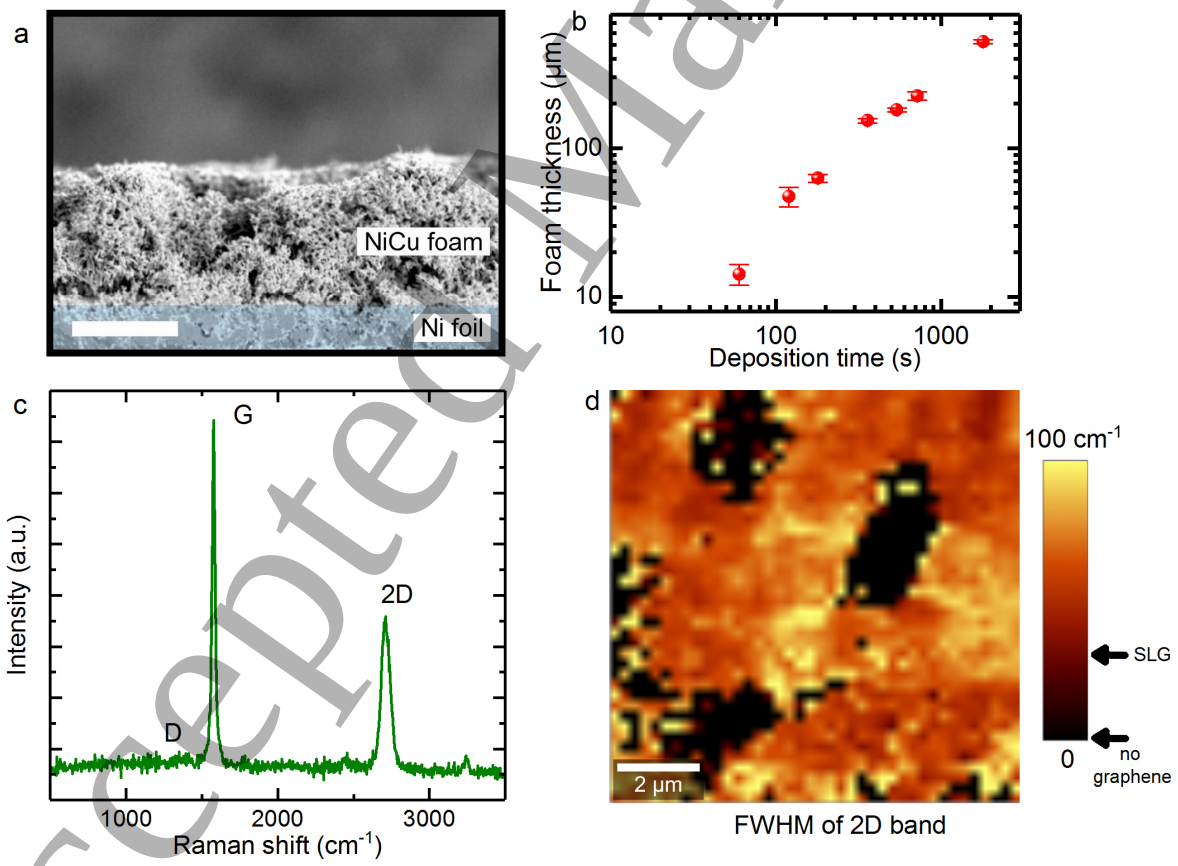

Figure 2. (a) SEM micrograph showing a cross-section of a NiCu alloy foam on a Ni foil (blue shaded) after graphene growth. The electrodeposition time of this metal foam was 6 minutes and the scale bar is 100 µm. (b) Thickness of the metal foam, measured using SEM images after graphene growth, as a function of the electrodeposition time. (c) Raman spectrum measured on a metal/graphene foam before Ni etching. (d) Raman map showing the FWHM of the 2D band revealing the porous structure.

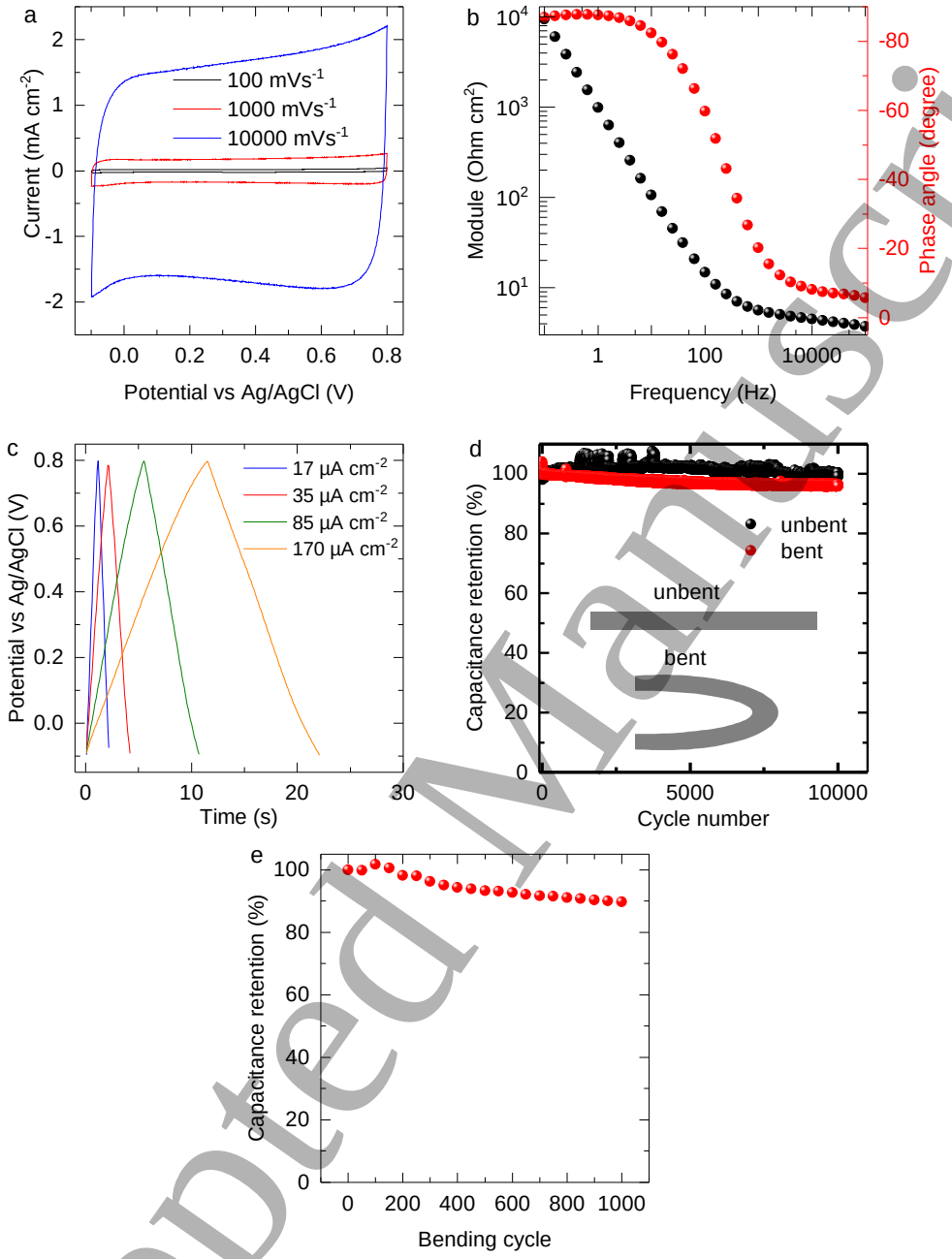

Figure 3. Electrochemical characterization of µGFs prepared using a metal foam substrate electrodeposited for 5 minutes (thickness ≈ 140 µm). (a) Cyclic voltammetry (CV) curves for three different scan rate, measured in a 3 M KCl aqueous electrolyte. (b) Corresponding electrochemical impedance spectrum (EIS) showing the module (black) and the phase (red) at a DC potential of 0.3 V vs Ag/AgCl. (c) Charge-discharge curves for four different current densities. (d) Capacitance retention of a µGF as a function of the cycle number measured in an unbent (black) and bent state (red). (e) Evolution of the capacitance of a µGF undergoing 1000 bending cycles. In all bending experiments, the bending radius is 6.5 mm.

saturation value of the module of the impedance at high frequencies and is $\approx 3.5\,\Omega\,\mathrm{cm}^2$. An investigation of its contributing components (see S.I. for more details) reveals a very low intrinsic resistance of the µGF, below $1.0\,\Omega\,\mathrm{cm}^2$. Charge-discharge (CD) curves (Fig. 3c) are characterized by a quasi-triangular shape, consistent with an almost ideal EDLC behavior. From the CD measurements, a volumetric specific capacitance of $18\,\mathrm{mF\,cm}^{-3}$ and an areal specific capacitance of $0.21\,\mathrm{mF\,cm}^{-2}$ can be obtained. Long-term experiments (Fig. 3d) show no capacitance loss after 10,000 cycles and reveal the excellent long time stability of the µGF. In the bent state, the capacitance decreases only 4 % after the same amount of CD cycles. The long-term mechanical stability is shown in Fig. 3e. After 1,000 bending cycles, where the sample was bent from an unbent state (0°) to a completely bent state (180°) with a bending radius of 6.5 mm, the capacitance of the µGF still has $\approx$ 90 % of its initial capacitance confirming the elastic strength of graphene[60]. We have not found any direct correlation between the mechanical stability and the investigated thicknesses of the µGFs (see Fig. 2b).

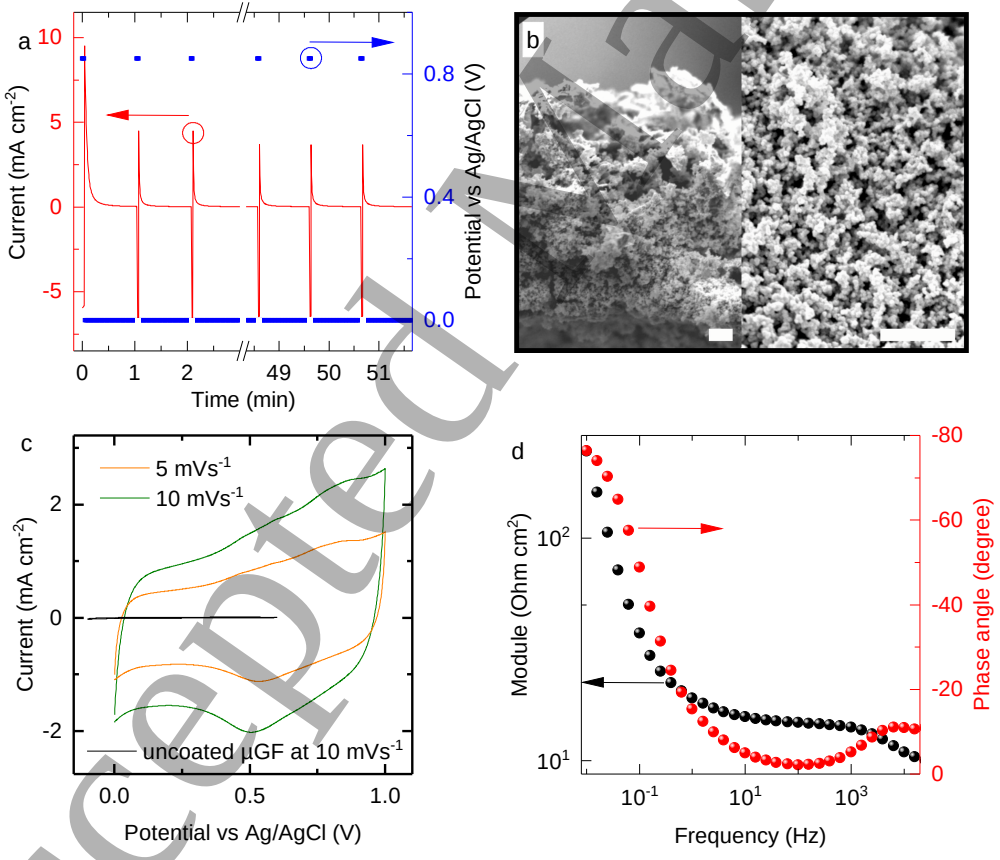

Figure 4. (a) Measured current density (red) during 50 potentiostatic pulses (blue) as a function of time in a 0.25 M manganese acetate electrolyte. (b) SEM images showing the µGF uniformly coated with manganese oxide. The scale bars are 5 µm. (c) CV curves of the MnO_2 coated µGF for two different scan rates in 1 M Na_2NO_3 and the corresponding EIS diagram (d) at a DC potential of 0.3 V vs Ag/AgCl.

The µGFs are then used as substrates for the electrodeposition of manganese oxide,

a pseudocapacitively active material. In order to achieve a uniform coating of the µGF current collector with manganese oxide, square wave potential pulses[61] in an electrolyte containing manganese acetate[62] have been used. Conventional reported coating techniques such as potentiostatic or galvanostatic electrodeposition[32] can not be applied since they do not consider the porous structure of the µGFs (see Fig. S10). Fig. 4a shows the recorded current (red curve) during 50 potential pulses at 0.85 V vs Ag/AgCl[63] (blue curve) for 2 s each followed by a 60 s period at 0.0 V vs Ag/AgCl. The resulting duty cycle of 1/30 has been tuned to the porous structure and the thickness of the graphene current collector. Higher duty cycles have been found to lead to an incomplete deposition of manganese in the interior pores and to clogging of the pores near the electrolyte bulk (see S.I.). The optimum number of pulses was found to be 50 considering the gain in capacitance, mass loading, and the ESR. The current peaks at the beginning of each potential pulse have contributions from the capacitive charging of the electrode, the deposition of manganese, and the oxidation of pre-deposited material. The current evolution after the pulse results from the capacitive discharging of the surface and the reduction of the electrochemically active material[64]. SEM is used to investigate the structure of the MnO_2 coating (Fig. 4b). A cross-section SEM image of the manganese coated µGF (Fig. 4b (left)) reveals no irregularities in the manganese deposition, i.e. both the top and bottom regions are covered with manganese oxide. As a result of the deposition by square wave potential pulses, the manganese oxide grows with a microspherical morphology (hundreds of nm in diameter in a $\approx 1\,\mu m$ thick layer) on the µGF substrate, thus forming additional pores in the sub-micrometer regime and increasing the surface area (see Fig. S9 for more SEM images). The additional gain in capacitance can be observed in the CV curves (Fig. 4c), where the current at $10\,mV\,s^{-1}$ at e.g. 0.5 V vs Ag/AgCl increases from $1\,\mu A\,cm^{-2}$ before manganese deposition to more than $1\,mA\,cm^{-2}$ after deposition. The CV curve shows the characteristic shape of the pseudocapacitive MnO_2[18] resulting from the combined effect of the adsorption of sodium ions from the electrolyte on the MnO_2 surface and the intercalation of sodium within the bulk of MnO_2[65]. Due to the very large increase in capacitance, the characteristic frequency of the µGF now coated with MnO_2 decreases to $\approx 0.1\,Hz$ (see Fig. 4d). The second peak observed in the phase angle at $\approx 5\,kHz$ represents a second time constant tentatively attributed to the MnO_2-covered multilayer graphene which serves as the substrate (see Methods). The capacitance values calculated from CD curves (see S.I.) are $14\,F\,cm^{-3}$ and $0.16\,F\,cm^{-2}$ and show a 10^3-fold increase with respect to the non-coated µGF.

The MnO_2-coated µGF can be used as the cathode in an asymmetric supercapacitor. Since MnO_2 can be irreversibly changed at negative potentials vs Ag/AgCl and in order to extend the potential windows of the asymmetric supercapacitor, a non-coated EDLC-based graphene foam (GF) is used as the anode. The GFs are grown by CVD using metal powder as catalyst as reported previously[66] (see S.I. for electrochemical characterization) and are much thicker ($\approx 5\,mm$) than the µGFs. Thus, their electric double layer capacitance is higher than that of a bare µGF and comparable with the

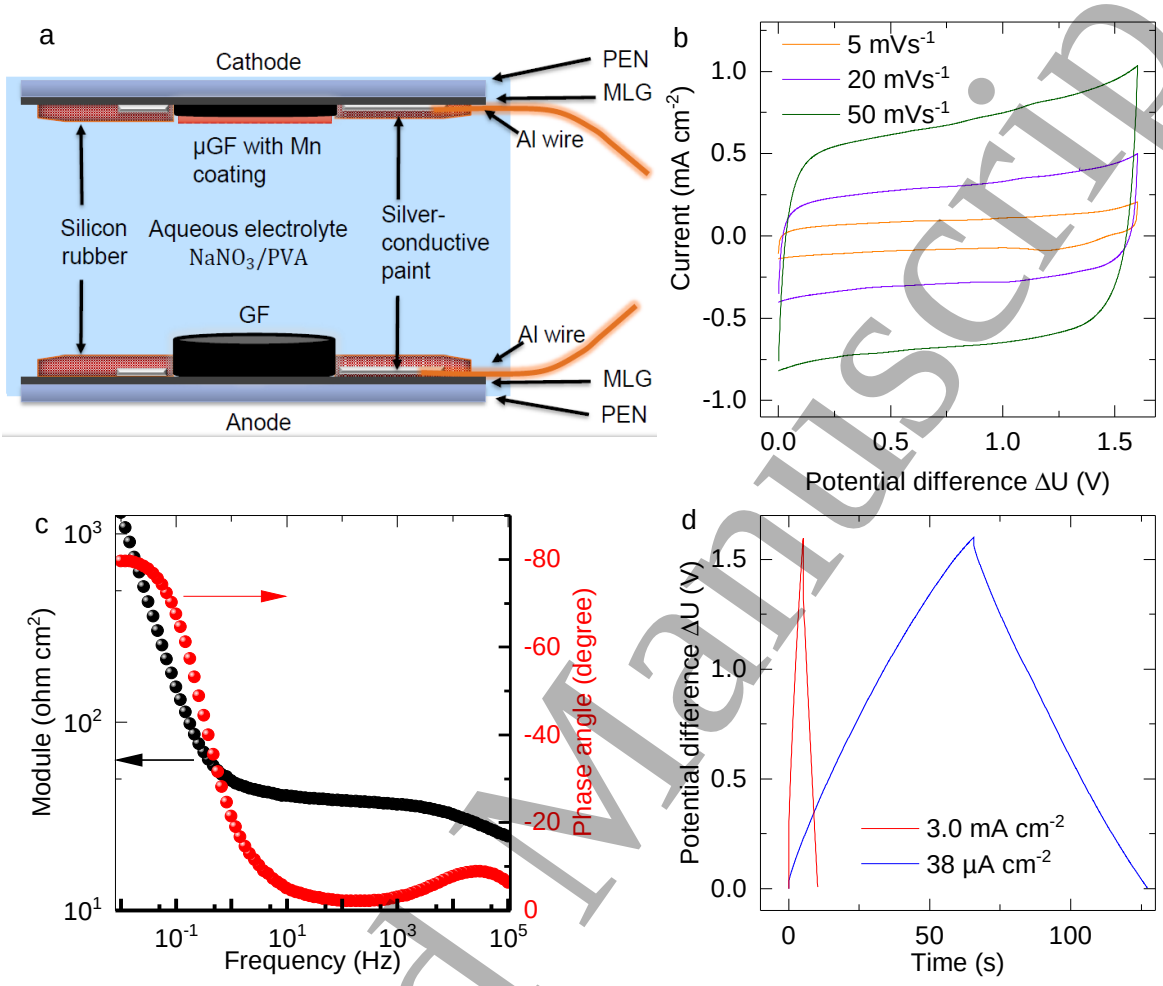

Figure 5. (a) Schematic of the asymmetric supercapacitor consisting of a MnO_2 coated µGF as anode (bottom) and a non-coated bare graphene foam (GF) as cathode (top). (b) Cyclic voltammetry curves of the asymmetric supercapacitor in polyvinyl alcohol (PVA) and 2 M $NaNO_3$. (c) the corresponding EIS spectrum for a DC potential of 0.0 V vs Ag/AgCl, and (d) charge-discharge (CD) curves. The electrochemical measurements were recorded in a bent state with a bending radius of 6.5 mm.

capacitance of a MnO_2-coated µGF. The method using copper powder as catalyst cannot be used for the growth of µGFs as a slight variation in the distribution of particles and a rough surface of the combustion vessel typically leads to the breakage of the copper foam after growth. Both electrodes are contacted with multilayer graphene (MLG), a conductive and chemically inert substrate, transferred onto polyethylene naphthalate (PEN) (Fig. 5a) assuring the flexibility of the asymmetric supercapacitor. Polyvinyl alcohol (PVA) and $NaNO_3$ serve both as separator and as conductive electrolyte, respectively. Fig. 5b-d show the electrochemical measurements of the flexible supercapacitor recorded in a bent state with a bending radius of 6.5 mm. The quasi-rectangular shape of the CV curves (Fig. 5b) without any peak due to a dominant chemical reaction can still be observed within a greater potential window of 1.6 V. The

ESR which is now the sum of the ESR of both electrodes and the resistance of the electrolyte between the electrodes is $\approx 38\,\Omega\,\mathrm{cm}^2$ (Fig. 5c). Yet, the characteristic frequency of the device is $\approx 0.3\,\mathrm{Hz}$ and indicates the possibility of fast charging and discharging of the supercapacitor. This is confirmed by CD experiments (Fig. 5d) where the quasi-triangular shape is maintained even at high current densities (red curve), resulting in a charge time of $\approx 5\,\mathrm{s}$, typical for a supercapacitor. The iR-drop (potential drop or rise at the beginning of each charging or discharging) remains nearly negligible for both current densities. The total capacitance of the device is $15\,\mathrm{mF\,cm^{-2}}$, which corresponds to the two capacitors in series ($C_{total} = \frac{C_1 C_2}{C_1+C_2}$). The capacitance of the EDLC-based cathode is about one fifth of the capacitance of the pseudocapacitive anode, assuring a very good long-term stability (Fig. S12) with a capacitance loss of only 1 % after 10,000 CD cycles.

3. Conclusion

We have demonstrated the fabrication of highly conductive porous thin-film graphene foams grown by CVD which can be used as current collector in flexible asymmetric supercapacitors after being uniformly coated with manganese dioxide. The metal catalyst used for the growth of graphene is fabricated using the anodic deposition of Ni and Cu on Ni foil, resulting in NiCu alloy foam with a thickness in the micrometer range which can be controlled by the duration of the electrodeposition. After graphene growth, the removal of the metal, and the transfer onto flexible PEN substrates, a highly conductive flexible graphene foam with high structural quality consisting of few layer graphene is obtained, exhibiting pores in the micrometer and sub-micrometer range. In contrast to other techniques where reduced graphene oxide sheets are pressed to a three-dimensional structure, the excellent electrical properties of the µGFs, resulting from the high crystalline quality of the film produced by CVD, lead to very low intrinsic resistances which can be observed in the quasi-rectangular shape of the CV curves even at very high scan rates up to $10\,\mathrm{V\,s^{-1}}$ and in the outstanding long-term and mechanical stability. The as-obtained µGFs can be used as current collector after coating them with manganese dioxide, a pseudocapacitive material. A uniform coverage is achieved using square wave voltammetry with duty cycles optimized for the porous structure and the thickness of the µGF. Following this approach, the capacitance of the electrode can be increased by more than three orders of magnitude from $18\,\mathrm{mF\,cm^{-3}}$ to $14\,\mathrm{F\,cm^{-3}}$. This electrode is used as cathode in a flexible graphene-based asymmetric supercapacitor using a bare graphene foam as anode showing an excellent long term performance with a capacitance loss of only 1 % after 10,000 cycles. This work can be used as a base for the development of flexible supercapacitors using a highly conductive thin-film micro graphene network, with pores and thickness in the micrometer regime, as current collector. The presented preparation technique for MnO_2 is of high relevance for coating three-dimensional networks containing micrometer-sized pores with electrochemically active materials. In contrast to previously reported supercapacitors[37, 38, 39, 40, 41],

the electrodes fabricated using our method combine the most important requirements for real application such as lateral and vertical scalability, flexibility, high energy density due to a uniform coverage with a pseudocapacitive material, and a high power density owing to the low intrinsic resistance of the electrode and especially of the current collector.

4. Methods

Fabrication of micro graphene foams

The metal substrate used for the growth of the µGFs serving as cathode was prepared by potentiostatic electrodeposition of Ni and Cu[42] on a Ni foil (thickness 25 µm, Alfa Aesar) at 3.0 V in an aqueous electrolyte consisting of 0.5 M $NiSO_4 \cdot 7H_2O$, 0.01 M $CuSO_4$, 1.5 M H_2SO_4, and 1 M HCl, resulting in a current density of 1.1 A cm^{-2}. The concentrations were optimized to obtain the foam structure with smallest pores and, in turn, highest surface area. The thickness of the as-produced NiCu alloy was controlled by the duration of the electrodeposition. The typical size of the GF is 1 x 2 cm^2. For the graphene growth, the metal substrates are placed into a horizontal tube furnace and heated up to 800 °C under a gas flow of 400 sccm argon and 100 sccm hydrogen at 200 mbar within 20 minutes. Following this so-called annealing step, an additional methane flow of 10 sccm is introduced to provide the carbon source for graphene growth. After 30 minutes, the samples are removed from the oven and cooled down to room temperature with a cooling rate of 6 °C s^{-1}.

Fabrication of graphene foams

The metal substrate used for the growth of the graphene serving as anode was obtained by filling copper powder (Sigma Aldrich, particle size between 0.5 and 1.5 µm) mixed with $MgCO_3$ powder into a quartz Petri dish as discussed elsewhere [66]. The graphene growth conditions were as detailed above except for a higher growth temperature of 950 °C, a lower growth pressure of 50 mbar, and a longer annealing step (60 minutes).

Foam transfer

To remove the metal, both types of samples are put into an etching solution of 1 M $FeCl_3$ and 2 M HCl for $\approx$ 6 hours. The etchant can enter the metal template through defects in the graphene layer(s) such as vacancies and grain boundaries. Etching residues are removed in two additional cleaning baths in 1 M HCl and deionized water.

Electrode Fabrication

Polyethylene naphthalate (PEN, thickness 125 µm) and multilayer graphene sheets (MLGs, typical size 2 x 3 cm^2) served as substrates for both electrodes (anode and cathode). MLGs were grown by CVD on Ni foil at 900 °C similar to the growth of the GFs and transferred onto PEN. Aluminum wires and silver paste were used to contact

the MLGs. After the transfer of the GFs onto the substrate, the wiring was insulated with silicone rubber to prevent contact with the electrolyte. The electrochemical measurements of single electrodes were recorded by a Parstat 2263 (Princeton Applied Technologies) using a three electrode system with a platinum mesh as counter electrode and a Ag/AgCl reference electrode.

Deposition of Manganese Dioxide

The µGFs were coated with manganese dioxide using potential pulses in an 0.5 M manganese acetate solution (Sigma Aldrich). 50 potential pulses at 0.85 V vs Ag/AgCl were applied, each lasting two seconds followed by a 60 seconds break. Afterwards, the samples were submerged in 0.05 M $KMnO_4$ for one hour and cleaned in deionized water.

Raman spectroscopy

Raman maps were acquired using an excitation wavelength of 532 nm. Using a 100x objective and measuring four spectra per micron allows a spatial resolution down to 250 nm. The D, G, and 2D peaks were fitted with Lorentzian functions; the intensity ratio is obtained from the fitted areas.

Supercapacitor Fabrication

The asymmetric capacitors (GF as anode and a manganese dioxide coated µGF as cathode) were covered and separated by an ionic gel consisting of polyvinyl alcohol and 2 M $NaNO_3$. The electrochemical measurements were recorded by a Gamry Reference 600 potentiostat in a two electrode configuration.

5. Acknowledgements

This work has been partially supported by the German Research Foundation (DFG) in the framework of the Priority Program 1459 Graphene, the Nanosystems Initiative Munich (NIM), and the European Unions H2020 Research and Innovation programme under Grant Agreement No. 696656 GrapheneCore1.

6. References

[1] Patrice Simon and Yury Gogotsi. Materials for electrochemical capacitors. *Nature materials*, 7(11):845–854, 2008.

[2] Max Lu. *Supercapacitors: Materials, Systems, and Applications*. Materials for sustainable energy and development. Wiley, Weinheim, 2013.

[3] B. E. Conway. Transition from "Supercapacitor" to "Battery" Behavior in Electrochemical Energy Storage. *Journal of The Electrochemical Society*, 138(6):1539, 1991.

[4] Huanwen Wang, Huan Yi, Xiao Chen, and Xuefeng Wang. Asymmetric supercapacitors based on nano-architectured nickel oxide/graphene foam and hierarchical porous nitrogen-doped carbon nanotubes with ultrahigh-rate performance. *J. Mater. Chem. A*, 2(9):3223–3230, 2014.

[5] Hongcai Gao, Fei Xiao, Chi Bun Ching, and Hongwei Duan. Flexible all-solid-state asymmetric supercapacitors based on free-standing carbon nanotube/graphene and Mn3O4 nanoparticle/graphene paper electrodes. *ACS applied materials & interfaces*, 4(12):7020–7026, 2012.

[6] Yuxi Xu, Zhaoyang Lin, Xiaoqing Huang, Yuan Liu, Yu Huang, and Xiangfeng Duan. Flexible solid-state supercapacitors based on three-dimensional graphene hydrogel films. *ACS nano*, 7(5):4042–4049, 2013.

[7] Jie Yang, Lifang Lian, Hongcheng Ruan, Fengyan Xie, and Mingdeng Wei. Nanostructured porous MnO2 on Ni foam substrate with a high mass loading via a CV electrodeposition route for supercapacitor application. *Electrochimica Acta*, 136:189–194, 2014.

[8] Jung Joon Yoo, Kaushik Balakrishnan, Jingsong Huang, Vincent Meunier, Bobby G. Sumpter, Anchal Srivastava, Michelle Conway, Arava Leela Mohana Reddy, Jin Yu, Robert Vajtai, and Pulickel M. Ajayan. Ultrathin planar graphene supercapacitors. *Nano letters*, 11(4):1423–1427, 2011.

[9] Haichao Chen, Jianjun Jiang, Li Zhang, Dandan Xia, Yuandong Zhao, Danqing Guo, Tong Qi, and Houzhao Wan. In situ growth of NiCo2S4 nanotube arrays on Ni foam for supercapacitors: Maximizing utilization efficiency at high mass loading to achieve ultrahigh areal pseudocapacitance. *Journal of Power Sources*, 254:249–257, 2014.

[10] Maher F. El-Kady, Veronica Strong, Sergey Dubin, and Richard B. Kaner. Laser scribing of high-performance and flexible graphene-based electrochemical capacitors. *Science (New York, N.Y.)*, 335(6074):1326–1330, 2012.

[11] Montree Sawangphruk, Pattarachai Srimuk, Poramane Chiochan, Atiweena Krittayavathananon, Santamon Luanwuthi, and Jumras Limtrakul. High-performance supercapacitor of manganese oxide/reduced graphene oxide nanocomposite coated on flexible carbon fiber paper. *Carbon*, 60:109–116, 2013.

[12] Marcos Ghislandi, Evgeniy Tkalya, Bernardo Marinho, Cor E. Koning, and Gijsbertus de With. Electrical conductivities of carbon powder nanofillers and their latex-based polymer composites. *Composites Part A: Applied Science and Manufacturing*, 53:145–151, 2013.

[13] Bernardo Marinho, Marcos Ghislandi, Evgeniy Tkalya, Cor E. Koning, and Gijsbertus de With. Electrical conductivity of compacts of graphene, multi-wall carbon nanotubes, carbon black, and graphite powder. *Powder Technology*, 221:351–358, 2012.

[14] Ying Tao, Xiaoying Xie, Wei Lv, Dai-Ming Tang, Debin Kong, Zhenghong Huang, Hirotomo Nishihara, Takafumi Ishii, Baohua Li, Dmitri Golberg, Feiyu Kang, Takashi Kyotani, and Quan-Hong Yang. Towards ultrahigh volumetric capacitance: Graphene derived highly dense but porous carbons for supercapacitors. *Scientific reports*, 3:2975, 2013.

[15] Yongmin He, Wanjun Chen, Xiaodong Li, Zhenxing Zhang, Jiecai Fu, Changhui Zhao, and Erqing Xie. Freestanding three-dimensional graphene/MnO2 composite networks as ultralight and flexible supercapacitor electrodes. *ACS nano*, 7(1):174–182, 2013.

[16] Yizhu Xie, Yan Liu, Yuda Zhao, Yuen Hong Tsang, Shu Ping Lau, Haitao Huang, and Yang Chai. Stretchable all-solid-state supercapacitor with wavy shaped polyaniline/graphene electrode. *J. Mater. Chem. A*, 2(24):9142–9149, 2014.

[17] Xin-hui Yang, Yong-gang Wang, Huan-ming Xiong, and Yong-yao Xia. Interfacial synthesis of porous MnO2 and its application in electrochemical capacitor. *Electrochimica Acta*, 53(2):752–757, 2007.

[18] Fang Xiao and Youlong Xu. Pulse electrodeposition of manganese oxide for high-rate capability supercapacitors. *Int. J. Electrochem. Sci*, 7(8):7440–7450, 2012.

[19] Yongfu Qiu, Pingru Xu, Bing Guo, Zhiyu Cheng, Hongbo Fan, Minlin Yang, Xiaoxi Yang, and Jianhui Li. Electrodeposition of manganese dioxide film on activated carbon paper and its application in supercapacitors with high rate capability. *RSC Adv*, 4(109):64187–64192, 2014.

[20] Sang Ha Lee, Hyuck Lee, Mi Suk Cho, Jae-Do Nam, and Youngkwan Lee. Morphology and composition control of manganese oxide by the pulse reverse electrodeposition technique for

high performance supercapacitors. *J. Mater. Chem. A*, 1(46):14606, 2013.

[21] A. Bello, K. Makgopa, M. Fabiane, D. Dodoo-Ahrin, K. I. Ozoemena, and N. Manyala. Chemical adsorption of NiO nanostructures on nickel foam-graphene for supercapacitor applications. *Journal of Materials Science*, 48(19):6707–6712, 2013.

[22] Nguyen van Hoa, Charmaine Lamiel, Nguyen Huu Nghia, Pham Anh Dat, and Jae-Jin Shim. Different morphologies of MnO 2 grown on the graphene@nickel foam electrode for supercapacitor application. *Materials Letters*, 208:102–106, 2017.

[23] Cuimei Zhao, Xin Wang, Shumin Wang, Yayu Wang, Yunxiao Zhao, and Weitao Zheng. Synthesis of Co(OH)2/graphene/Ni foam nano-electrodes with excellent pseudocapacitive behavior and high cycling stability for supercapacitors. *International Journal of Hydrogen Energy*, 37(16):11846–11852, 2012.

[24] Guoyin Zhu, Zhi He, Jun Chen, Jin Zhao, Xiaomiao Feng, Yanwen Ma, Quli Fan, Lianhui Wang, and Wei Huang. Highly conductive three-dimensional MnO2-carbon nanotube-graphene-Ni hybrid foam as a binder-free supercapacitor electrode. *Nanoscale*, 6(2):1079–1085, 2014.

[25] Xinhui Xia, Jiangping Tu, Yongjin Mai, Rong Chen, Xiuli Wang, Changdong Gu, and Xinbing Zhao. Graphene sheet/porous NiO hybrid film for supercapacitor applications. *Chemistry (Weinheim an der Bergstrasse, Germany)*, 17(39):10898–10905, 2011.

[26] Umakant Patil, Su Chan Lee, Sachin Kulkarni, Ji Soo Sohn, Min Sik Nam, Suhyun Han, and Seong Chan Jun. Nanostructured pseudocapacitive materials decorated 3D graphene foam electrodes for next generation supercapacitors. *Nanoscale*, 7(16):6999–7021, 2015.

[27] U. M. Patil, Su Chan Lee, J. S. Sohn, S. B. Kulkarni, K. V. Gurav, J. H. Kim, Jae Hun Kim, Seok Lee, and Seong Chan Jun. Enhanced Symmetric Supercapacitive Performance of Co(OH)2 Nanorods Decorated Conducting Porous Graphene Foam Electrodes. *Electrochimica Acta*, 129:334–342, 2014.

[28] Yaming Wang, Junchen Chen, Jianyun Cao, Yan Liu, Yu Zhou, Jia-Hu Ouyang, and Dechang Jia. Graphene/carbon black hybrid film for flexible and high rate performance supercapacitor. *Journal of Power Sources*, 271:269–277, 2014.

[29] Huiqing Fan, Lixia Quan, Mengqi Yuan, Shasha Zhu, Kai Wang, Yuan Zhong, Ling Chang, Haibo Shao, Jianming Wang, Jianqing Zhang, and Chu-nan Cao. Thin Co 3 O 4 nanosheet array on 3D porous graphene/nickel foam as a binder-free electrode for high-performance supercapacitors. *Electrochimica Acta*, 188:222–229, 2016.

[30] Abdulhakeem Bello, Omobosede O. Fashedemi, Joel N. Lekitima, Mopeli Fabiane, David Dodoo-Arhin, Kenneth I. Ozoemena, Yury Gogotsi, Alan T. Charlie Johnson, and Ncholu Manyala. High-performance symmetric electrochemical capacitor based on graphene foam and nanostructured manganese oxide. *AIP Advances*, 3(8):082118, 2013.

[31] Xinhui Xia, Dongliang Chao, Zhanxi Fan, Cao Guan, Xiehong Cao, Hua Zhang, and Hong Jin Fan. A new type of porous graphite foams and their integrated composites with oxide/polymer core/shell nanowires for supercapacitors: Structural design, fabrication, and full supercapacitor demonstrations. *Nano letters*, 14(3):1651–1658, 2014.

[32] Qing Chen, Yuning Meng, Chuangang Hu, Yang Zhao, Huibo Shao, Nan Chen, and Liangti Qu. MnO2-modified hierarchical graphene fiber electrochemical supercapacitor. *Journal of Power Sources*, 247:32–39, 2014.

[33] Cao Guan, Xianglin Li, Zilong Wang, Xiehong Cao, Cesare Soci, Hua Zhang, and Hong Jin Fan. Nanoporous walls on macroporous foam: Rational design of electrodes to push areal pseudocapacitance. *Advanced materials (Deerfield Beach, Fla.)*, 24(30):4186–4190, 2012.

[34] Y. F. Yuan, X. H. Xia, J. B. Wu, J. L. Yang, Y. B. Chen, and S. Y. Guo. Nickel foam-supported porous Ni(OH)2/NiOOH composite film as advanced pseudocapacitor material. *Electrochimica Acta*, 56(6):2627–2632, 2011.

[35] Chongyang Yang, Jiali Shen, Chunyan Wang, Haojie Fei, Hua Bao, and Gengchao Wang. All-solid-state asymmetric supercapacitor based on reduced graphene oxide/carbon nanotube and carbon fiber paper/polypyrrole electrodes. *J. Mater. Chem. A*, 2(5):1458–1464, 2014.

[36] Kwang Hoon Lee, Young-Woo Lee, Seung Woo Lee, Jeong Sook Ha, Sang-Soo Lee, and Jeong Gon Son. Ice-templated Self-assembly of VOPO4-Graphene Nanocomposites for Vertically Porous 3D Supercapacitor Electrodes. *Scientific reports*, 5:13696, 2015.

[37] Qiong Wu, Yuxi Xu, Zhiyi Yao, Anran Liu, and Gaoquan Shi. Supercapacitors based on flexible graphene/polyaniline nanofiber composite films. *ACS nano*, 4(4):1963–1970, 2010.

[38] Aaron Davies, Philippe Audette, Blake Farrow, Fathy Hassan, Zhongwei Chen, Ja-Yeon Choi, and Aiping Yu. Graphene-Based Flexible Supercapacitors: Pulse-Electropolymerization of Polypyrrole on Free-Standing Graphene Films. *The Journal of Physical Chemistry C*, 115(35):17612–17620, 2011.

[39] Junfeng Xie, Xu Sun, Ning Zhang, Kun Xu, Min Zhou, and Yi Xie. Layer-by-layer b-Ni(OH)2/graphene nanohybrids for ultraflexible all-solid-state thin-film supercapacitors with high electrochemical performance. *Nano Energy*, 2(1):65–74, 2013.

[40] Yimin Sun, Zheng Fang, Chenxu Wang, K. R. Rakhitha Malinga Ariyawansha, Aijun Zhou, and Hongwei Duan. Sandwich-structured nanohybrid paper based on controllable growth of nanostructured MnO2 on ionic liquid functionalized graphene paper as a flexible supercapacitor electrode. *Nanoscale*, 7(17):7790–7801, 2015.

[41] Zan Gao, Wanlu Yang, Jun Wang, Ningning Song, and Xiaodong Li. Flexible all-solid-state hierarchical NiCo2O4/porous graphene paper asymmetric supercapacitors with an exceptional combination of electrochemical properties. *Nano Energy*, 13:306–317, 2015.

[42] S. Eugénio, T. M. Silva, M. J. Carmezim, R. G. Duarte, and M. F. Montemor. Electrodeposition and characterization of nickel–copper metallic foams for application as electrodes for supercapacitors. *Journal of Applied Electrochemistry*, 44(4):455–465, 2014.

[43] Jeong-Han Kim, Ryoung-Hee Kim, and Hyuk-Sang Kwon. Preparation of copper foam with 3-dimensionally interconnected spherical pore network by electrodeposition. *Electrochemistry Communications*, 10(8):1148–1151, 2008.

[44] Blake J. Plowman, Lathe A. Jones, and Suresh K. Bhargava. Building with bubbles: the formation of high surface area honeycomb-like films via hydrogen bubble templated electrodeposition. *Chemical communications (Cambridge, England)*, 51(21):4331–4346, 2015.

[45] Alfonso Reina, Xiaoting Jia, John Ho, Daniel Nezich, Hyungbin Son, Vladimir Bulovic, Mildred S. Dresselhaus, and Jing Kong. Large area, few-layer graphene films on arbitrary substrates by chemical vapor deposition. *Nano letters*, 9(1):30–35, 2009.

[46] Ivan Vlassiouk, Murari Regmi, Pasquale Fulvio, Sheng Dai, Panos Datskos, Gyula Eres, and Sergei Smirnov. Role of hydrogen in chemical vapor deposition growth of large single-crystal graphene. *ACS nano*, 5(7):6069–6076, 2011.

[47] Xuesong Li, Yanwu Zhu, Weiwei Cai, Mark Borysiak, Boyang Han, David Chen, Richard D. Piner, Luigi Colombo, and Rodney S. Ruoff. Transfer of large-area graphene films for high-performance transparent conductive electrodes. *Nano letters*, 9(12):4359–4363, 2009.

[48] Xuesong Li, Weiwei Cai, Luigi Colombo, and Rodney S. Ruoff. Evolution of graphene growth on Ni and Cu by carbon isotope labeling. *Nano letters*, 9(12):4268–4272, 2009.

[49] HoKwon Kim, Cecilia Mattevi, M. Reyes Calvo, Jenny C. Oberg, Luca Artiglia, Stefano Agnoli, Cyrus F. Hirjibehedin, Manish Chhowalla, and Eduardo Saiz. Activation energy paths for graphene nucleation and growth on Cu. *ACS nano*, 6(4):3614–3623, 2012.

[50] Maria Losurdo, Maria Michela Giangregorio, Pio Capezzuto, and Giovanni Bruno. Graphene CVD growth on copper and nickel: role of hydrogen in kinetics and structure. *Physical chemistry chemical physics : PCCP*, 13(46):20836–20843, 2011.

[51] Francesco Bonaccorso, Antonio Lombardo, Tawfique Hasan, Zhipei Sun, Luigi Colombo, and Andrea C. Ferrari. Production and processing of graphene and 2d crystals. *Materials Today*, 15(12):564–589, 2012.

[52] G. A. López and E. J. Mittemeijer. The solubility of C in solid Cu. *Scripta Materialia*, 51(1):1–5, 2004.

[53] J. J. Lander, H. E. Kern, and A. L. Beach. Solubility and Diffusion Coefficient of Carbon in

Nickel: Reaction Rates of Nickel–Carbon Alloys with Barium Oxide. *Journal of Applied Physics*, 23(12):1305–1309, 1952.

[54] Stephan Hofmann, Philipp Braeuninger-Weimer, and Robert S. Weatherup. CVD-Enabled Graphene Manufacture and Technology. *The journal of physical chemistry letters*, 6(14):2714–2721, 2015.

[55] A. C. Ferrari and J. Robertson. Interpretation of Raman spectra of disordered and amorphous carbon. *Physical Review B*, 61(20):14095–14107, 2000.

[56] Andrea C. Ferrari and Denis M. Basko. Raman spectroscopy as a versatile tool for studying the properties of graphene. *Nature nanotechnology*, 8(4):235–246, 2013.

[57] S. Das Sarma, Shaffique Adam, E. H. Hwang, and Enrico Rossi. Electronic transport in two-dimensional graphene. *Reviews of Modern Physics*, 83(2):407–470, 2011.

[58] E. H. Hwang, S. Adam, and S. Das Sarma. Carrier transport in two-dimensional graphene layers. *Physical review letters*, 98(18):186806, 2007.

[59] Mark E. Orazem and Bernard Tribollet. *Electrochemical Impedance Spectroscopy*. John Wiley & Sons, Inc, Hoboken, NJ, USA, 2008.

[60] Changgu Lee, Xiaoding Wei, Jeffrey W. Kysar, and James Hone. Measurement of the elastic properties and intrinsic strength of monolayer graphene. *Science (New York, N.Y.)*, 321(5887):385–388, 2008.

[61] G. Moses Jacob and I. Zhitomirsky. Microstructure and properties of manganese dioxide films prepared by electrodeposition. *Applied Surface Science*, 254(20):6671–6676, 2008.

[62] Qinghua Huang, Xianyou Wang, and Jun Li. Characterization and performance of hydrous manganese oxide prepared by electrochemical method and its application for supercapacitors. *Electrochimica Acta*, 52(4):1758–1762, 2006.

[63] Tong Xue, Cai-Ling Xu, Dan-Dan Zhao, Xiao-Hong Li, and Hu-Lin Li. Electrodeposition of mesoporous manganese dioxide supercapacitor electrodes through self-assembled triblock copolymer templates. *Journal of Power Sources*, 164(2):953–958, 2007.

[64] Huanwen Wang, Yalan Wang, and Xuefeng Wang. Pulsed laser deposition of large-area manganese oxide nanosheet arrays for high-rate supercapacitors. *New Journal of Chemistry*, 37(4):869, 2013.

[65] Weifeng Wei, Xinwei Cui, Weixing Chen, and Douglas G. Ivey. Manganese oxide-based materials as electrochemical supercapacitor electrodes. *Chemical Society reviews*, 40(3):1697–1721, 2011.

[66] Simon Drieschner, Michael Weber, Jörg Wohlketzetter, Josua Vieten, Evangelos Makrygiannis, Benno M. Blaschke, Vittorio Morandi, Luigi Colombo, Francesco Bonaccorso, and Jose A. Garrido. High surface area graphene foams by chemical vapor deposition. *2D Materials*, 3(4):045013, 2016.